Uplink-Aided Downlink Channel Estimation for a High-Mobility Massive MIMO-OTFS System

Daidong Ying*, Feng Ye*, Rose Qingyang Hu†, and Yi Qian‡
*Department of Electrical and Computer Engineering, University of Dayton, Dayton, OH, USA
† Department of Electrical and Computer Engineering, Utah State University, Logan, UT, USA
‡ Department of Electrical and Computer Engineering, University of Nebraska-Lincoln, Omaha, NE, USA
Emails: yingd1@udayton.edu, fye001@udayton.edu, rose.hu@usu.edu, yi.qian@unl.edu

GLOBECOM 2022 - 2022 IEEE Global Communications Conference | 978-1-6654-3540-6/22/$31.00 ©2022 IEEE | DOI: 10.1109/GLOBECOM48099.2022.10001420

***Abstract*—The massive multi-input-multi-output (MIMO) system will greatly enhance the performance of the next-generation wireless communications for many applications e.g., high-mobility users. The orthogonal time frequency space (OTFS) is a promising technique for high-mobility massive MIMO use cases. However, the MIMO-OTFS system requires accurate downlink channel information for optimal performance. This paper studies an uplink-aided downlink channel estimation scheme targeting high-mobility user scenario based on a frequency division duplex massive MIMO-OTFS system. Most of the existing work overlooks the change in the delay, Doppler, and angle domain during a channel estimation process due to high mobility. In this work, we analyze the reciprocity between an uplink and a downlink channel and derive the estimation error due to the latency in processing the uplink channel estimates. Simulation results demonstrate that an uplink channel may change significantly in a high-mobility massive MIMO-OTFS system, given a reasonably small amount of processing latency. Such a change will lead to high error in downlink channel estimation. With the proof of concept, our future work will focus on refining the channel estimation framework with a reduction of the processing latency.**

I. INTRODUCTION

The future wireless communications will support various high-mobility use cases, such as connected vehicles, high-speed railways, unmanned autonomous vehicles, etc [1]. The current mobile network is mainly developed based on the orthogonal frequency division multiplexing (OFDM). However, in a high mobility environment, the OFDM channel can be fast time-varying due to Doppler frequency offsets. The existing Doppler compensation schemes on the OFDM channel may introduce high complexity to a communication system [2]. The complexity could be further exacerbated in a massive multiple-input-multi-output (MIMO) system. Recently, orthogonal time frequency space (OTFS) is proposed to deal with the fast time-varying channels with much less complexity [3]. Technically, OTFS transforms a time-varying multi-path channel into a 2-D channel in the delay-Doppler domain. All symbols experience the same channel gain so that the full diversity can be extracted [4, 5]. In a massive MIMO-OTFS system, a channel from the delay-Doppler domain is extended to the angle (space) domain with a sparse 3-D structure. To enhance the spectrum efficiency of the OTFS system, the downlink channel state information (CSI) is required for both the receiver and the transmitter [6]. However, a direct CSI estimation by solving a sparse signal recovery problem could introduce a high computational cost and a large training overhead.

978-1-6654-3540-6/22/$31.00 © 2022 IEEE

To tackle this issue, in this paper, we study an uplink-aided downlink channel estimation framework for a high-mobility massive MIMO-OTFS system. Without loss of generality, a frequency division duplex (FDD) system is considered in this work. Uplink-aided downlink channel estimation has been widely studied for FDD MIMO systems [7], as well as the massive MIMO-OTFS system [8]. To estimate a downlink channel, the uplink CSI is first estimated. After analyzing the reciprocity of the uplink channel and downlink channel, the parameters in uplink channel estimation can assist the downlink CSI estimation. A future massive MIMO system with a large antenna array and ultra high carrier frequency will have very high resolutions in the channel domains, e.g., delay and angle. For example, in the high frequency band, e.g., 40 GHz, the system whose sub-channel bandwidth is 375 KHz, the sampling clock rate reaches 768 MHz [9]. Therefore, the physical movement of a high-mobility user during the channel estimation may cause a significant change in the actual CSI. However, such latency during the uplink and downlink CSI estimation is not considered in those existing uplink-aided downlink channel estimation schemes.

This work considers such a latency in the studied FDD massive MIMO-OTFS system framework. Specifically, an orthogonal matching pursuit (OMP) based uplink channel estimation scheme is first studied. The sudden channel changes due to the shift of delay and Doppler indices from high mobility are analyzed. After estimating the uplink channel, the resource block for the downlink will be coded at the transmitter (i.e., base station). The pilot symbols and the data symbols will be coded into the same resource block [10]. Different from the traditional downlink channel estimation scheme that every user has its dedicated pilot block, our scheme uses a common pilot area to reduce the pilot overhead. Each user configures its own pilot region in every angle domain by using the indices of the paths provided in the uplink channel estimation. Based on the pilot regions and the received signal, the downlink channel can be estimated using existing methods, e.g., Least Square (LS) method [11]. The shift of the pilot region in the downlink estimation is analyzed based on the index changes from the uplink estimation. Simulations are conducted to demonstrate the studied framework and the impact from index changes

Authorized licensed use limited to: University of Dayton Libraries. Downloaded on January 23,2023 at 03:23:20 UTC from IEEE Xplore. Restrictions apply.

on the overall channel estimation. The rest of the paper is organized as follows. In section II, the system model and OTFS transmission are introduced. In section III, the OMP based uplink channel estimation is first introduced, followed by the reciprocity analysis, and the proposed downlink channel estimation and resource block coding schemes. In section IV, the simulation results are demonstrated. In Section V, the conclusion is given.

II. System Model

In this paper, we study an FDD massive MIMO-OTFS system in high mobility environment. As shown in Fig. 1, the base station is equipped with a Uniform Linear Array (ULA) contains M antennas. Each user device is equipped with a single antenna. Assuming that the system is deployed in a multi-path propagation environment, where each user may receive signals from multiple scatter clusters. Meanwhile, the scatter clusters may create multiple paths to different users [12]. Without loss of generality, assume that there are P paths for the k-th user. Then the steering vector of p-th path is denoted as:

$$\mathbf{a}(\theta_{k,p}) = [1, e^{-j2\pi\frac{x\cos\theta_{k,p}}{\lambda}}, \ldots, e^{-j2\pi(M-1)\frac{x\cos\theta_{k,p}}{\lambda}}], \quad (1)$$

where x is the distance between the adjacent antennas in the antenna array; λ is the wave-length of the carrier frequency; and $\theta_{k,p}$ is the Angle of Departure (AoD) of p-th path.

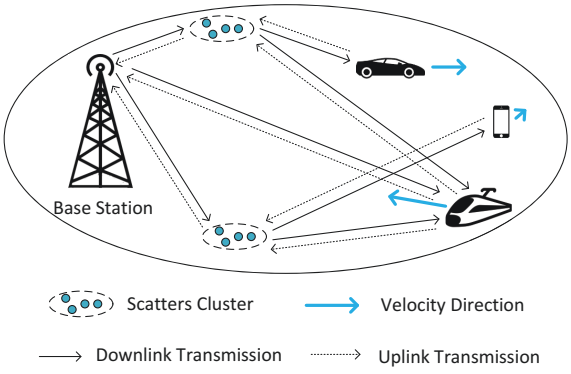

Figure 1. Massive MIMO-OTFS system with high-mobility users.

For better illustration, we assume that the data bits are mapped into data symbols by using some constellation, e.g., 4-QAM. These symbols are placed into a 3-D, i.e., delay, Doppler shift, and angle (DDA), data block $\mathbf{X}^{\text{DDA}}$. The length of these 3 dimensions are L, D and M, respectively. In practice, the data block needs to be transformed into the time-frequency-space (TFS) domain s.t.,

$$\mathbf{X}^{\text{FTS}}[l', d', m'] = \frac{1}{\sqrt{LDM}} \sum_{l=0}^{L-1}\sum_{d=0}^{D-1}\sum_{m=0}^{M-1} \mathbf{X}^{\text{DDA}}[l, d, m] e^{j2\pi(\frac{dd'}{D} - \frac{ll'}{L} - \frac{mm'}{M})}, \quad (2)$$

where l, d and m are the indices on the DDA domains; and l', d' and m' are the indices on the FTS domains, respectively. Let $L \times D$ matrix $\mathbf{X}^{\text{FTS}}[:, :, m']$ denote the 2-D data matrix sent by the $m'+1$-th antenna in the time-frequency domain. Then the data in $\mathbf{X}^{\text{FTS}}_{m'}$ can be converted into a continuous waveform by using Heisenberg transform [3] as follows:

$$s_{m'}(t) = \sum_{l'=0}^{L-1}\sum_{d'=0}^{D-1} \mathbf{X}^{\text{FTS}}[l', d', m'] g_{tx}(t - d'T_s) e^{j2\pi l'\Delta f(t-d'T_s)}, \quad (3)$$

where $g_{tx}(t)$ is a pulse-shaping filter of the transmitter; $T_s = \frac{1}{L\Delta f}$ is the sampling time of the system; $\Delta f = \frac{1}{DT_s}$ is the frequency resolution. The waveform will be transmitted through the multi-path channel. The received signal at the receiver is denoted as:

$$r_{m'}(t) = \int\int h_{m'}(\tau, \nu) s_{m'}(t-\tau) e^{j2\pi\nu(t-\tau)} \mathrm{d}\tau \mathrm{d}\nu + n_{m'}(t), \quad (4)$$

where $n_{m'}(t)$ is the additional white Gaussian noise; $h_{m'}(\tau, \nu)$ is the channel of $m'+1$-th antenna who has a sparse representation [13] as:

$$h_{m'}(\tau, \nu) = \sum_{p=1}^{P} h_p \delta(\tau - \tau_p)\delta(\nu - \nu_p)\mathbf{a}(\theta_p)[m'], \quad (5)$$

where h_p, τ_p and ν_p are the path gain, delay, and Doppler shift of p-th path, respectively; $\mathbf{a}(\theta_p)[m']$ is the $m'+1$-th element in $\mathbf{a}(\theta_p)$; and $\delta(\cdot)$ denotes the Dirac delta function. Similar to [8], we assume that each scatter path corresponds to a unique AoD, time delay and Doppler shift. The delay of p-th path is an integer multiples of the delay resolution, s.t. $\tau_p = l_p T_s$. The Doppler shift of p-th path is denoted as $\nu_p = \frac{d_p}{DT_s}$.

The receiver transfers the time-serial received data to the frequency-time domain by using Wigner transform, s.t.,

$$\mathbf{Y}^{\text{FTS}}[l', d', m'] = \int r_{m'}(t) g^*_{rx}(t - d'T_s) e^{-j2\pi l'\Delta f(t-d'T_s)} \mathrm{d}t, \quad (6)$$

where $(\cdot)^*$ denotes the complex conjugate. Assume that the $g_{tx}(t)$ and $g_{rx}(t)$ are ideal waveforms, i.e., by satisfying the bi-orthogonal property:

$$\int g_{tx}(t - dT_s) e^{j2\pi l\Delta f(t-dT_s)} g^*_{tx}(t - d'T_s) \times e^{-j2\pi l'\Delta f(t-d'T_s)} \mathrm{d}t = \delta[d - d']\delta[l - l']. \quad (7)$$

The signal in time-frequency domain is then transformed into the delay-Doppler domain as follows:

$$\mathbf{Y}^{\text{DDS}}[l, d, m'] = \frac{1}{\sqrt{LD}} \sum_{l'=0}^{L-1}\sum_{d'=0}^{D-1} \mathbf{Y}^{\text{FTS}}[l', d', m'] e^{j2\pi(\frac{ll'}{L} - \frac{dd'}{D})}. \quad (8)$$

The final received signal is the summation of the signals from all transmitting antennas, s.t., $\mathbf{Y}^{\text{DD}}[l, d] = \sum_{m'=1}^{M} \mathbf{Y}^{\text{DDS}}[l, d, m']$. By summarizing the aforementioned

Authorized licensed use limited to: University of Dayton Libraries. Downloaded on January 23,2023 at 03:23:20 UTC from IEEE Xplore. Restrictions apply.

equations from Eq. (2) to Eq. (8), we can acquire the input-output relation in the delay-Doppler domain as follows:

$$\begin{aligned}\mathbf{Y}^{\mathrm{DDS}}[l,d,m'] = \frac{1}{LD}\sum_{q=0}^{L-1}\sum_{r=0}^{D-1}\mathbf{X}^{\mathrm{DDS}}[q,r,m'] \\ \times \mathbf{H}^{\mathrm{DDS}}[l-q,d-r,m'] + \omega[l,d,m'],\end{aligned} \tag{9}$$

where $\omega[l,d,m']$ is the corresponding noise of $\mathbf{Y}^{\mathrm{DDS}}[l,d,m']$; $\mathbf{X}^{\mathrm{DDS}}$ is the data matrix after performing DFT in the angle domain of $\mathbf{X}^{\mathrm{DDA}}$. The effective channel in the delay-Doppler domain is denoted as:

$$\begin{aligned}&\mathbf{H}^{\mathrm{DDS}}[\tau,\nu,m'] \\ &= \int_{\nu'}\int_{\tau'} h(\tau',\nu')\Big[\sum_{l'=0}^{L-1}\sum_{d'=0}^{D-1} e^{j2\pi l'\Delta f(\tau-\tau')}e^{j2\pi d' T_s(\nu'-\nu)}\Big] \\ &\times e^{-j2\pi\nu'\tau'}\mathrm{d}\tau'\mathrm{d}\nu' e^{-2\pi m'\frac{x\cos\theta_p}{\lambda}},\end{aligned} \tag{10}$$

where $\tau = \frac{l-q}{L\Delta f}$, for $0 \le l \le L-1$ and $0 \le q \le L-1$; l is the index of the received data matrix on the delay domain; q is the index of the transmitted data matrix on the delay domain. Meanwhile, $\nu = \frac{d-r}{DT_s}$ for $0 \le d \le D-1$ and $0 \le r \le D-1$, where d is the index of the received data matrix on the Doppler domain, and r is the index of the transmitted data matrix on the Doppler domain. The delay-Doppler domain channel has a peak value at $\nu = \frac{d-r}{DT_s} = \nu' = \frac{d_p}{DT_s}$ and $\tau = \frac{l-q}{L\Delta f} = \tau' = \frac{l_p}{L\Delta f}$ [13]. Without loss of generality, we assume that there is only one significant value is located in the peak, i.e., $d-r = d_p$ and $l-q = l_p$. The received signal in Eq. (9) can be further denoted as:

$$\begin{aligned}&\mathbf{Y}^{\mathrm{DDS}}[l,d,m'] \\ &\approx \sum_{p=1}^{P} h_p e^{-j2\pi\tau_p\nu_p}\mathbf{X}^{\mathrm{DDS}}[[l-l_p]_L,[d-d_p]_D,m'] \\ &\times e^{-2\pi m'\frac{x\cos\theta_p}{\lambda}} + \omega[l,d,m'],\end{aligned} \tag{11}$$

where $[\cdot]_L$ represents $mod\ L$ operation. After stacking all the channels in the delay-Doppler-space domain into a 3-D channel, we have $\mathbf{H}^{\mathrm{DDS}} \in \mathbb{C}^{l_{\max}\times(2d_{\max}+1)\times M}$, where $l_{\max}$ is the largest delay index, $d_{\max}$ is the largest absolute value of all d_p. And we have $-d_{\max} \le d_p \le d_{\max}$ and $0 \le l_p \le l_{\max}-1$. To transform the channel into the DDA domain, one can perform the IDFT along the antenna index m' as follows:

$$\mathbf{H}^{\mathrm{DDA}}[l,d,m] = \frac{1}{\sqrt{M}}\sum_{m'=0}^{M-1}\mathbf{H}^{\mathrm{DDS}}[l,d,m']e^{j2\pi\frac{mm'}{M}}. \tag{12}$$

Different from the space domain, the channel has sparsity in the angle domain. Following the analysis above, we can see that $\mathbf{H}^{\mathrm{DDA}}$ has the dominant value at $l = l_p$, $d = d_p$ and $m = \lfloor M\frac{\theta_p}{\pi}\rceil$, where $\lfloor\cdot\rceil$ is the round function.

III. Uplink-aided Downlink Channel Estimation

In the studied massive MIMO-OTFS system, the base station requires the parameter set $\{\tau_p,\nu_p,\theta_p,h_p\}_{p=1}^{P}$ to design a precoder. However, direct estimation of the downlink channel would need some powerful sparse signal recovery methods with high computation burden and large training overhead [8]. The uplink-aided approach can significantly reduce the complexity in the downlink channel estimation by exploring the DDA reciprocity between the uplink and downlink.

A. Uplink Channel Estimation

In the uplink channel, the users first send the pilots to the base station. Assume that K users send the pilot sequences simultaneously. Let the pilot matrix sent by k-th user in the delay-Doppler space be $\mathbf{P}_k^{\mathrm{DD}} \in \mathbb{C}^{Q\times R}$. Usually, the size of the pilot matrix is much smaller than the full size of a resource block, i.e., $Q \le L$ and $R \le D$. The rest of the grids are the transmitted data symbols. For better illustration, we assume that the whole resource block is used as a pilot in the rest of this subsection. At the base station, the received signal is in TFS domain. The signal can be transformed into the DDA domain by using the inverse process of Eq. (2). Due to page limit, this step is not presented here. Then the received signal of the m-th angle at the base station can be denoted as:

$$\begin{aligned}\mathbf{Z}_m^{\mathrm{DDA}}[l,d,m] = \sum_{k=1}^{K}\sum_{l^{\mathrm{up}}=0}^{l_{\max}-1}\sum_{d^{\mathrm{up}}=-d_{\max}}^{d_{\max}}\overline{\mathbf{H}}_{k,m}^{\mathrm{DDA}}[l^{\mathrm{up}},d^{\mathrm{up}},m] \\ \times \mathbf{P}_k^{\mathrm{DD}}[[l-l^{\mathrm{up}}]_L,[d-d^{\mathrm{up}}]_D] + \omega[l,d,m],\end{aligned} \tag{13}$$

where $\omega[l,d,m]$ is the corresponding noise of $\mathbf{Z}_m^{\mathrm{DDA}}[l,d,m]$; and $\overline{\mathbf{H}}_{k,m}^{\mathrm{DDA}}$ is the uplink channel in delay-Doppler-angle domain of k-th user. Without loss of generality, if the k-th user has no dominant channel gain in m-th angle, we assume that $\overline{\mathbf{H}}_{k,m}^{\mathrm{DDA}} = \mathbf{0}$, where $\mathbf{0}$ denotes the all zeros. Then we write Eq. (13) into the vector-matrix form, where $\mathbf{Z}_m^{\mathrm{DDA}}$ is arranged into a column vector $\mathbf{z}_m \in \mathbb{C}^{LD\times 1}$. The $lD+d+1$-th element of $\mathbf{z}_m$ is $\mathbf{Z}_m^{\mathrm{DDA}}[l,d,m]$, where $0 \le l \le L-1$, $0 \le d \le D-1$. Accordingly, $\overline{\mathbf{H}}_{k,m}^{\mathrm{DDA}}$ is also arranged into a vector $\mathbf{h}_{k,m} \in \mathbb{C}^{l_{\max}D_\nu\times 1}$, where $D_\nu = 2d_{\max}+1$. Assume that the users have the same $l_{\max}$ and D_ν. The $(l^{\mathrm{up}}D_\nu + d^{\mathrm{up}} + d_{\max}+1)$-th element of $\mathbf{h}_{k,m}$ is equal to $\overline{\mathbf{H}}_{k,m}^{\mathrm{DDA}}[l^{\mathrm{up}},d^{\mathrm{up}},m]$, where $0 \le l^{\mathrm{up}} \le l_{\max}-1$, and $-d_{\max} \le d^{\mathrm{up}} \le d_{\max}$. Then Eq. (13) can be written as:

$$\mathbf{z}_m = \sum_{k=1}^{K}\widetilde{\mathbf{P}}_k^{\mathrm{DD}}\mathbf{h}_{k,m} + \boldsymbol{\omega}_m, \tag{14}$$

where $\widetilde{\mathbf{P}}_k^{\mathrm{DD}} \in \mathbb{C}^{LD\times l_{\max}D_\nu}$ is the 2-D convolution matrix, where $\widetilde{\mathbf{P}}_k^{\mathrm{DD}}[lD+d, l^{\mathrm{up}}D_\nu + d^{\mathrm{up}} + d_{\max}]$ is equal to $\mathbf{P}[l-l^{\mathrm{up}}, d-d^{\mathrm{up}}]$. Then Eq. (14) can be further written as:

$$\mathbf{z}_m = \overline{\mathbf{P}}^{\mathrm{DD}}\mathbf{h}_m + \boldsymbol{\omega}_m, \tag{15}$$

where $\overline{\mathbf{P}}^{\mathrm{DD}} = [\widetilde{\mathbf{P}}_1^{\mathrm{DD}},...,\widetilde{\mathbf{P}}_K^{\mathrm{DD}}] \in \mathbb{C}^{LD\times Kl_{\max}D_\nu}$ and $\mathbf{h}_m = [\mathbf{h}_{1,m}^T,...,\mathbf{h}_{K,m}^T]^T \in \mathbb{C}^{Kl_{\max}D_\nu\times 1}$. In this way, the channel estimation problem can be formulated as M sparse signal recovery problems in M angle domains with the same sensing matrix $\boldsymbol{\Psi} = \overline{\mathbf{P}}^{\mathrm{DD}}$ [6], which can be solved by the OMP algo-

Authorized licensed use limited to: University of Dayton Libraries. Downloaded on January 23,2023 at 03:23:20 UTC from IEEE Xplore. Restrictions apply.

rithm in [11, 14]. First, we define the residual measurements in m-th angle domain as:

$$\mathbf{r}_m = \mathbf{z}_m - \mathbf{\Psi}\hat{\mathbf{h}}_m^{(i)}, \tag{16}$$

where $\hat{\mathbf{h}}_m^{(i)}$ is the estimated channel in i-th iteration, and $\mathbf{h}_m^{(0)}$ denotes the initial CSI estimate. Meanwhile, an index set $\Lambda_m = \emptyset$ is also initialized. The detail of the proposed uplink CSI estimation scheme is presented in Alg. 1.

Assume that the average number of users share m-th angle domain can be acquired statistically as K_m. In step 6 of the algorithm, $\mathbf{\Psi}^{\dagger}_{(\Lambda^{(i)})} = (\mathbf{\Psi}^H_{(\Lambda^{(i)})}\mathbf{\Psi}_{(\Lambda^{(i)})})^{-1}\mathbf{\Psi}^H_{(\Lambda^{(i)})}$, $(\cdot)^H$ is the Hermitian transpose. According to the locations of non-zero elements in $\mathbf{h}_m$, the indices in the delay domain and Doppler domain of k-th user can be found. Specifically, $k = \mathcal{Q}(\eta, l_{\max}D_\nu) + 1$, where $\mathcal{Q}(a, b)$ denotes the quotient of modular operation of a and b. $l^{\text{ul}}_{k,m} = \mathcal{Q}(\mathcal{R}(\eta, l_{\max}D_\nu), D_\nu)$, where $\mathcal{R}(a, b)$ denote the reminder of modular operation of a and b. And $d^{\text{ul}}_{k,m} = \mathcal{R}(\mathcal{R}(\eta, l_{\max}D_\nu), D_\nu) - d_{\max}$. The channel gain $h^{\text{ul}}_{k,m}$ is acquired in step 6. Then we have the parameters set for p-th path of k-th user as $\{l^{\text{ul}}_{k,m}, d^{\text{ul}}_{k,m}, m, h_{k,m}\}_p$. Once all the M sparse signal recovery problems are solved by Algorithm 1, we have the uplink parameter set $\{\tau^{\text{ul}}_{k,p}, \nu^{\text{ul}}_{k,p}, \theta^{\text{ul}}_{k,p}, h^{\text{ul}}_{k,p}\}_{p=1}^P, k = 1, \ldots, K$.

Algorithm 1 OMP-based uplink channel estimation

Input: Measurements $\mathbf{z}_m$, Sensing matrix $\mathbf{\Psi}$;
Output: Estimated channel $\hat{\mathbf{h}}_m$;
1: **Initialize:**
$i = 1$; $\Lambda_m^{(0)} = \emptyset$; $\mathbf{h}_m^{(0)} = \mathbf{0}$;
2: **while** $i \leq K_m$ **do**
3: $\mathbf{r}_m = \mathbf{z}_m - \mathbf{\Psi}\hat{\mathbf{h}}_m^{(i-1)}$;
4: $\eta^{(i)} = \arg \max_{j=1,\ldots,Kl_{\max}D_\nu} |\mathbf{r}_m^H \mathbf{\Psi}[:, j]|$;
5: $\Lambda^{(i)} = \Lambda^{(i-1)} \cup \eta^{(i)}$;
6: $\hat{\mathbf{h}}_m[\Lambda^{(i)}] = \mathbf{\Psi}^{\dagger}_{(\Lambda^{(i)})}\mathbf{z}_m$;
7: $i = i + 1$;
8: **end while**

B. Reciprocity between Uplink and Downlink Channels

In an FDD massive MIMO-OTFS system, the parameter set that acquired in uplink estimation cannot be used directly for downlink CSI estimation. Nonetheless, the uplink and downlink share the same propagation space, thus the spatial reciprocity holds. The delay and angle of the downlink channel can be directly acquired as $\tau^{\text{dl}}_{k,p} = \tau^{\text{ul}}_{k,p}$ and $\theta^{\text{dl}}_{k,p} = \theta^{\text{ul}}_{k,p}$, respectively. Since the uplink channel and downlink channel are in different carrier frequency, the Doppler shift needs to be transferred as $\nu^{\text{dl}}_{k,p} = f^{\text{dl}}\nu^{\text{ul}}_{k,p}/f^{\text{ul}}$, where f^{dl} is the carrier frequency of the downlink and f^{ul} is the carrier frequency of the uplink. And downlink channel gains cannot be directly inferred from the uplink channel gains.

For high-mobility users, the propagation environment may change significantly between the uplink and downlink channel estimations. Assume that the user sends its uplink pilot sequence at T_0. The signal is received by the base station antenna array after a propagation delay $\tau^{\text{ul}}_{k,p}$. Then the base station will estimate the uplink channel by the approach described in the previous subsection. The base station will also design the pilot matrix based on the result of the uplink estimation. This processing delay between receiving the uplink pilot signal and transmitting the downlink signal is denoted as T_p. After the additional downlink propagation delay $\tau^{\text{dl}}_{k,p}$, the user receives the downlink pilot sequence. It means the pilot indices used in downlink channel could have a significant latency between the real indices, s.t.,

$$\Delta\tau_{k,p} = \frac{1}{c}\left(\sqrt{s_k^2 + (\Delta s_k)^2 + 2s_k\Delta s_k \cos\phi_{k,p}} - s_k\right), \tag{17}$$

where s_k is the path length between the user and the scatter cluster at T_0; $\Delta s_k = v_k(\tau^{\text{up}}_{k,p} + T_p + \tau^{\text{dl}}_{k,p})$; v_k is the velocity of the k-th user; $\phi_{k,p}$ is the angle between the AoA and the moving direction. In practice, the processing delay T_p dominates the propagation delays $\tau^{\text{dl}}_{k,p}$ and $\tau^{\text{ul}}_{k,p}$. For simplicity, the scatters are assumed to be relatively static. Therefore, the movement of the users only cause angle change in the Line of Sight (LoS) path, s.t.,

$$\Delta\theta_{k,p} = \tan^{-1}\left(\frac{\Delta s_k \sin\phi_{k,p}}{s_k + \Delta s_k \cos\phi_{k,p}}\right). \tag{18}$$

Although the users' velocity is relatively steady during $\Delta\tau$, the angle between AoA and the moving direction might still change unless the direction of movement aligns with the AoA. Then the Doppler change is denoted as:

$$\Delta\nu_{k,p} = \frac{f_k}{c}\left(v_k \cos\phi_{k,p} - v_k \cos\phi'_{k,p}\right), \tag{19}$$

where $\phi'_{k,p}$ is the angle between the AoA and the moving direction after $\tau^{\text{ul}}_{k,p} + T_p + \tau^{\text{dl}}_{k,p}$, f_k is the center frequency. It is worth noting that the coverage of the scatter clusters is limited. A user may not be covered by the current cluster after T_p. This change of path may also lead to significant channel changes. However, this is beyond the scope of this paper.

C. Downlink Channel Estimation

While the parameter set $\{\tau^{\text{dl}}_{k,p}, \nu^{\text{dl}}_{k,p}, \theta^{\text{dl}}_{k,p}\}_{p=1}^P$ of k-th user in the downlink channel can be estimated based on the uplink channel estimation and the reciprocity analysis, the path gain $h_{k,p}$ still needs to be estimated in the studied FDD massive MIMO-OTFS system. Given Eq. (11), the downlink data transmission of k-th user is denoted as:

$$\begin{aligned}\mathbf{Y}_k^{\text{DD}}[l, d] = &\sum_{p=1}^{P} \mathbf{H}^{\text{DDA}}[\hat{l}_{k,p}, \hat{d}_{k,p}, m_p] \\ &\times \mathbf{X}^{\text{DDA}}_{k,p}[[l - \hat{l}_{k,p}]_L, [d - \hat{d}_{k,p}]_D, m_p] + \omega[l, d],\end{aligned} \tag{20}$$

where $\mathbf{X}^{\text{DDA}}_{k,p}$ is the transmitted data matrix in the angle domain corresponding to the p-th path. $\hat{l}_{k,p}$ and $\hat{d}_{k,p}$ are the real delay index and Doppler index of the p-th path, calculated as:

$$\hat{l}_{k,p} = l_{k,p} + \frac{\Delta\tau_{k,p}}{T_s}, \quad \hat{d}_{k,p} = d_{k,p} + \frac{\Delta\nu_{k,p}}{\Delta f}. \tag{21}$$

Authorized licensed use limited to: University of Dayton Libraries. Downloaded on January 23,2023 at 03:23:20 UTC from IEEE Xplore. Restrictions apply.

The pilot region is denoted as $\mathcal{X}_{k,p} = \{(l,d)|l \in [q_{k,p}, q_{k,p} + L_{k,p} - 1], d \in [r_{k,p}, r_{k,p} + D_{k,p} - 1]\}$, where $L_{k,p}$ and $D_{k,p}$ are the lengths of the pilot matrix on the delay domain and Doppler domain, respectively. Then the observation region at the receiver side is denoted as $\mathcal{Y}_{k,p} = \{(l,d)|l \in [q'_{k,p}, q'_{k,p} + L_{k,p} - 1], d \in [r'_{k,p}, r'_{k,p} + D_{k,p} - 1]\}$, where $q'_{k,p} = q_{k,p} + \hat{l}_{k,p}$ and $r'_{k,p} = r_{k,p} + \hat{d}_{k,p}$. The observation region in all the angle domains of k-th user is the same which is denoted as $\mathcal{Y}_k$. Therefore, it is required that $q'_{k,1} = q'_{k,2} = \cdots = q'_{k,P}$ and $r'_{k,1} = r'_{k,2} = \cdots = r'_{k,P}$. With the received pilot sequence, the channel gain of the downlink paths can be estimated by the LS method [11]. Assuming P symbols are chosen in $\mathcal{Y}_k$ to estimate P unknown channel gains. Let the selected symbol set of k-th user be:

$$\mathbf{y}_k = \bar{\mathbf{X}}_k \mathbf{h}_k + \boldsymbol{\omega}_k, \tag{22}$$

where $\mathbf{y}_k$ is a $P \times 1$ vector that consists of P received data in the observation region; $\boldsymbol{\omega_k}$ is the noise vector; $\mathbf{h}_k$ is a $P \times 1$ vector, which $\mathbf{h}_k[p] = \mathbf{H}^{\text{DDA}}[l_{k,p}, d_{k,p}, m_p]$; $\bar{\mathbf{X}}_k$ is a $P \times P$ matrix contains elements in $\mathbf{X}^{\text{DDA}}_{k,p}, \forall p \in [1, \ldots, P]$. Assume that $\mathbf{Y}^{\text{DDA}}_k[l,d]$ is selected and arranged to the $i+1$-th position in $\mathbf{y}_k$. Then we have $\bar{\mathbf{X}}_k[i,p] = \mathbf{X}^{\text{DDA}}_{k,p}[[l - l_{k,p}]_L, [d - d_{k,p}]_D, m_p]$. Using the LS estimator, the channel gains can be calculated as:

$$\hat{\mathbf{h}}_k = \bar{\mathbf{X}}^{\dagger}_k \mathbf{y}_k. \tag{23}$$

However, according to Eq. (20), the real pilots at present should be $\mathbf{X}^{\text{DDA}}_{k,p}[[l - \hat{l}_{k,p}]_L, [d - \hat{d}_{k,p}]_D, m_p]$. Fig. 2 illustrates an example. This difference will lead to an estimation error. Without loss of generality, the normalized mean square error is used to measure the estimation error, s.t.,

$$\varepsilon = \frac{\sum_{p=1}^{P} |\hat{\mathbf{h}}_k[p] - \mathbf{h}_k[p]|}{\sum_{p=1}^{P} |\mathbf{h}_k[p]|}. \tag{24}$$

In the multi-user situation, the users who share the same angle domain would have overlapping pilot regions. The overlapped pilots grids can be used by these users [10]. Therefore, the number of total grids assigned to the pilots can be reduced if more pilot symbols are shared. In practice, the maximum delay and maximum Doppler shifts are relatively small compared with the scale of the resource block. For simplicity, one observation region is fixed for all the users, s.t. $\mathcal{Y} = \{(l,d)|l \in [q_o, q_o + L_o - 1], d \in [r_o, r_o + D_o - 1]\}$, where q_o and r_o are the smallest delay index and Doppler index respectively of the common observation region. $L_{k,p} = L_o, \forall k \in [1, ..., K], \forall p \in [1, ..., P]$ and $D_{k,p} = D_o, \forall k \in [1, ..., K], \forall p \in [1, ..., P]$ are the lengths of the pilot length on delay domain and Doppler domain respectively. Define the largest delay index among all the users as $L_{\max}$, and the largest Doppler shift index among all the users as $D_{\max}$. Then the pilot region in every angle domain is denoted as $\mathcal{P} = \{(l,d)|l \in [q_o - L_{\max}, q_o + L_o - 1], d \in [r_o - D_{\max}, r_o + D_{\max} + D_o - 1]\}$. To avoid interference from the pilot symbols to the data symbols, guard intervals are added as shown in Fig. 2. Note that this pilot region design only works for the situation that each path corresponds to a unique angle, time delay and Doppler. The proposed method will be further refined in the case where few significant values exist around the peak on the Doppler domain.

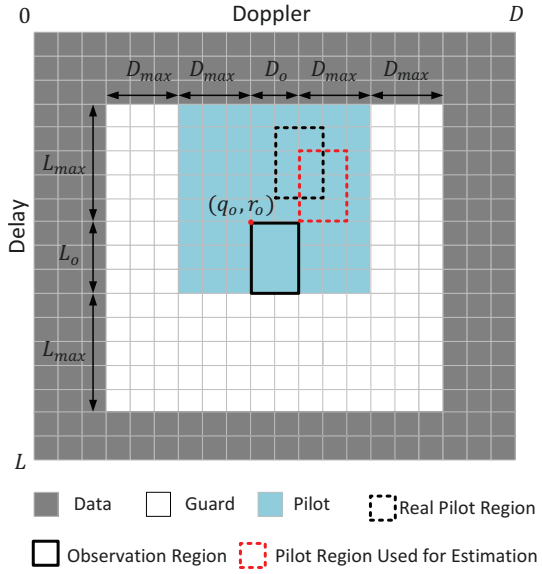

Figure 2. Illustration of proposed OTFS frame in one angle domain.

IV. Evaluation Results

Without loss of generality, the evaluations are conducted in the FDD massive MIMO-OTFS system. The users in the system locate within a circular area around the base station with a radius of 300 meters. The base station is equipped with 128 antennas and the users are equipped with 1 antenna each. The velocity of the users is 100 m/s. The center frequency of the system is 30 GHz. Therefore, the maximum Doppler shift and delay are 10 KHz and 3 μs respectively. The scatters in this network are assumed to be single-bounce. In this case, the average delay spread and delay are 1.7 μs and 2 μs respectively. Accordingly, the coherent bandwidth can be calculated as $f_c = \frac{1}{2 \times 1.7\ \mu\text{s}} = 294$ KHz. Assuming 64 sub-channels, where the bandwidth of each sub-channel is $B = 200$ KHz. In other words, the frequency width of one resource block is approximately 12.5 MHz, and the sampling time $T_s = 0.078$ μs. The time length of the resource block is 1 ms (i.e. $D = 12820$). The Doppler resolution is 1 KHz (i.e. $L = 12500$).

Fig. 3 shows the evaluation results of the uplink channel estimation. When $T_p = 0$, i.e., no latency, the locations of the significant channel elements in the delay-Doppler domain can be accurately recovered. When the latency is small compared to the resolutions in the delay-Doppler domain, e.g., $T_p = 1$ ms, the estimation of the significant channel elements can remain accurate. However, when the latency increases with a longer T_p, the physical movement of a high-mobility user will shift the locations of the significant channel elements in the delay-Doppler domain. The delay shift is caused mainly

Authorized licensed use limited to: University of Dayton Libraries. Downloaded on January 23,2023 at 03:23:20 UTC from IEEE Xplore. Restrictions apply.

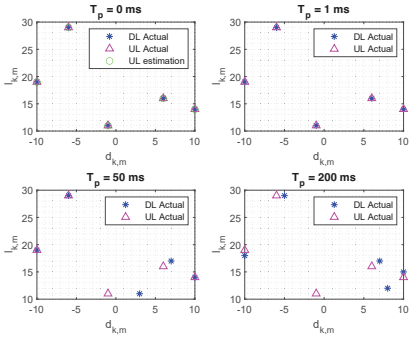

Figure 3. Simulation results of the uplink channel estimation and the real non-zero channel locations.

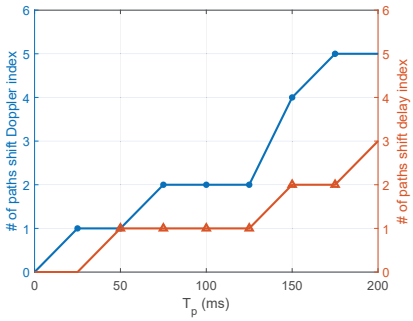

Figure 4. Evaluation results of changes indices in the uplink estimation.

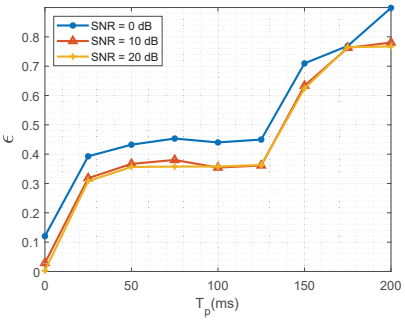

Figure 5. Evaluation results of the downlink channel estimation.

due to change of the path length. In this simulation, we assume that the cluster always cover the user. Consequently, the angle between the user movement and the AoA might change significantly when the user is close to the cluster. Therefore, the Doppler shifts when $T_p = 50$ ms and $T_p = 100$ ms are obvious in the evaluation results. In practice, the coverage area of the scatter clusters are limited. The movement of the user might lead to path changes, which may introduce additional shifts to the estimates. This path change will be explored in our future work. Fig. 4 shows the evaluation results of the index change for one user. We assume that the channel of this user consists of 5 paths. Then we count the number of the paths that changes the index in delay domain and Doppler domain respectively with different T_p. The simulation results shows that the longer T_p usually leads to more index shifts. Fig. 5 shows the evaluation results of the downlink channel estimation. For a given channel signal-to-noise ratio (SNR), the accuracy of downlink CSI depends on the accuracy of the uplink CSI monotonically. When an channel index shifts due to latency in the processing of uplink CSI, the elements in $\bar{\mathbf{X}}_k$ can not be correctly selected. Therefore, the downlink CSI $\hat{\mathbf{h}}_k$ would be different from the actual values. With increased latency, the estimation error becomes more significant.

V. Conclusion and Future Work

In this work, we studied an uplink-aided downlink channel estimation scheme for an FDD massive MIMO-OTFS system with high-mobility users. Due to the significant movement of high-mobility users, the latency between uplink estimate and downlink estimate was considered in the studied framework. The simulation results demonstrated that the uplink channel and downlink channel can be accurately estimated when the considered latency is low. However, when practical latency presents, the estimated downlink CSI can differ significantly from the actual values. In the future work, we will focus on improving the channel estimation scheme with the consideration of a practical latency between uplink and downlink estimates.

Acknowledgment

This work was partially supported by National Science Foundation under grants ECCS-2139569, ECCS-2139508, and ECCS-2139520.

Reference

[1] C.-X. Wang, J. Bian, J. Sun, W. Zhang, and M. Zhang, "A survey of 5g channel measurements and models," *IEEE Communications Surveys Tutorials*, vol. 20, no. 4, pp. 3142–3168, 2018.

[2] W. Guo, W. Zhang, P. Mu, F. Gao, and H. Lin, "High-mobility wideband massive mimo communications: Doppler compensation, analysis and scaling laws," *IEEE Transactions on Wireless Communications*, vol. 18, no. 6, pp. 3177–3191, 2019.

[3] R. Hadani, S. Rakib, M. Tsatsanis, A. Monk, A. J. Goldsmith, A. F. Molisch, and R. Calderbank, "Orthogonal time frequency space modulation," in *2017 IEEE Wireless Communications and Networking Conference (WCNC)*, 2017, pp. 1–6.

[4] G. Liu, A. Liu, R. Zhang, and M. Zhao, "Angular-domain selective channel tracking and doppler compensation for high-mobility mmwave massive mimo," *IEEE Transactions on Wireless Communications*, vol. 20, no. 5, pp. 2902–2916, 2021.

[5] H. Qu, G. Liu, L. Zhang, M. A. Imran, and S. Wen, "Low-dimensional subspace estimation of continuous-doppler-spread channel in otfs systems," *IEEE Transactions on Communications*, vol. 69, no. 7, pp. 4717–4731, 2021.

[6] W. Shen, L. Dai, J. An, P. Fan, and R. W. Heath, "Channel estimation for orthogonal time frequency space (otfs) massive mimo," *IEEE Transactions on Signal Processing*, vol. 67, no. 16, pp. 4204–4217, 2019.

[7] J. Guo, C.-K. Wen, and S. Jin, "Canet: Uplink-aided downlink channel acquisition in fdd massive mimo using deep learning," *IEEE Transactions on Communications*, vol. 70, no. 1, pp. 199–214, 2022.

[8] Y. Liu, S. Zhang, F. Gao, J. Ma, and X. Wang, "Uplink-aided high mobility downlink channel estimation over massive mimo-otfs system," *IEEE Journal on Selected Areas in Communications*, vol. 38, no. 9, pp. 1994–2009, 2020.

[9] *Numerology for new radio interface*. 3GPP document R1-162386, 2016.

[10] D. Shi, W. Wang, L. You, X. Song, Y. Hong, X. Gao, and G. Fettweis, "Deterministic pilot design and channel estimation for downlink massive mimo-otfs systems in presence of the fractional doppler," *IEEE Transactions on Wireless Communications*, vol. 20, no. 11, pp. 7151–7165, 2021.

[11] O. K. Rasheed, G. D. Surabhi, and A. Chockalingam, "Sparse delay-doppler channel estimation in rapidly time-varying channels for multiuser otfs on the uplink," in *2020 IEEE 91st Vehicular Technology Conference (VTC2020-Spring)*, 2020, pp. 1–5.

[12] L. Liu, C. Oestges, J. Poutanen, K. Haneda, P. Vainikainen, F. Quitin, F. Tufvesson, and P. D. Doncker, "The cost 2100 mimo channel model," *IEEE Wireless Communications*, vol. 19, no. 6, pp. 92–99, 2012.

[13] P. Raviteja, K. T. Phan, Y. Hong, and E. Viterbo, "Interference cancellation and iterative detection for orthogonal time frequency space modulation," *IEEE Transactions on Wireless Communications*, vol. 17, no. 10, pp. 6501–6515, 2018.

[14] J. A. Tropp and A. C. Gilbert, "Signal recovery from random measurements via orthogonal matching pursuit," *IEEE Transactions on Information Theory*, vol. 53, no. 12, pp. 4655–4666, 2007.

Authorized licensed use limited to: University of Dayton Libraries. Downloaded on January 23,2023 at 03:23:20 UTC from IEEE Xplore. Restrictions apply.